XXIV Italian Group of Fracture Conference, 1-3 March 2017, Urbino, Italy

A new advanced railgun system for debris impact study

A. Vricella*, A. Delfini, A. Pacciani, R. Pastore, D. Micheli,
G. Rubini, M. Marchetti, F. Santoni

Department of Astronautics, Electric and Energy Engineering, University Sapienza of Rome, via Eudossiana 18, 00184 Rome, Italy

Abstract

The growing quantity of debris in Earth orbit poses a danger to users of the orbital environment, such as spacecraft. It also increases the risk that humans or manmade structures could be impacted when objects reenter Earth's atmosphere. During the design of a spacecraft, a requirement may be specified for the surviv-ability of the spacecraft against Meteoroid / Orbital Debris (M/OD) impacts throughout the mission; further-more, the structure of a spacecraft is designed to insure its integrity during the launch and, if it is reusable, during descent, re-entry and landing. In addition, the structure has to provide required stiffness in order to allow for exact positioning of experiments and antennas, and it has to protect the payload against the space environment. In order to decrease the probability of spacecraft failure caused by M/OD, space maneuver is needed to avoid M/OD if the M/OD has dimensions larger than 10cm, but for M/OD with dimensions less than 1cm M/OD shields are needed for spacecrafts. It is therefore necessary to determine the impact-related failure mechanisms and associated ballistic limit equations (BLEs) for typical spacecraft components and subsys-tems. The methods that are used to obtain the ballistic limit equations are numerical simulations and la-borato-ry experiments. In order to perform an high energy ballistic characterization of layered structures, a new ad-vanced electro-magnetic accelerator, called railgun, has been assembled and tuned. A railgun is an electrically powered electromagnetic projectile launcher. Such device is made up of a pair of parallel conducting rails, which a sliding metallic armature is accelerated along by the electromagnetic effect (Lorentz force) of a cur-rent that flows down one rail, into the armature and then back along the other rail, thanks to a high power pulse given by a bank of capacitors. A tunable power supplier is used to set the capacitors charging voltage at the desired level: in this way the Rail Gun energy can be tuned as a function of the desired bullet velocity. This facility is able to analyze both low and high velocity impacts. A numerical simulation is also performed by using the Ansys Autodyn code in order to analyze the damage. The experimental results and numerical simulations show that the railgun-device is a good candidate to perform impact testing of materials in the space debris energy range.

---

* Corresponding author. Tel.: +39-349 4469058.
  E-mail address: antonio.vricella@uniroma1.it

1. Introduction

Since the beginning of space age on 4 October 1957 (launch of Sputnik I), there have been more than 4,900 space launches, leading to over 18,000 satellites and ground-trackable objects currently in Earth orbit. For each satellite launched, several other objects are also injected into orbit, including rocket upper stages, instrument covers, etc. This causes an uncontrolled growth of objects in orbital environment, see Schneider (1990) and McKnight (1991). Some catastrophic accident suggests the need to protect spacecrafts and satellites against M/OD impact (M/OD with dimensions less than 10 cm) that could damage and, in the worst case, destroy them as indicated by Piattoni et al. (2014), Pigliaru et al. (2014), Piergentili et al. (2014), Santoni et al. (2013). This protection could be assured by shielding technologies such as the Whipple Shield, a kind of shield that protects space structures against hypervelocity impacts as indicated by D. Palmieri, M. Faraud et al. (2001). It is therefore necessary to determine the impact-related failure mechanisms and associated ballistic limit equations (BLEs) for typical spacecraft components and subsystems as reported by Eric L. Christiansen, Justin H. Kerr (2001). The methods that are used to obtain the ballistic limit equations are laboratory experiments and numerical simulations as indicated by Faraud M, Destefanis (1999). To make ballistic tests it can use different methodologies depending on the energy of impact to be achieved ; for example, for low energies of impact Micheli D., Gradoni et al. (September 2010) and D.Micheli et al. (September 2011) performed ballistic tests using a coilgun. In order to perform an high energy ballistic characterization of layered structures, a new advanced electromagnetic accelerator called railgun, developed by Micheli et al. (2014, 2016), has been assembled and tuned. A railgun is an electrically powered electromagnetic projectile launcher. In this work, we demonstrate the possibility of using the railgun as a system for conducting hypervelocity impact tests. Numerical simulation and experimental tests were carried out on two types of shielding structure, an aluminum monolithic shield and a WS structure composed of an aluminum wall and a composite material bumper (multilayered structure).

Nomenclature	
BLE	Ballistic limit equations
BWS	Break Wire System
CFRP	Carbon Fiber Reinforced Materials
CNT	Carbon Nanotube
M/OD	Meteoroid / orbital debris
MWCNTs	Multiwall Carbon Nanotubes
RG	Railgun
WS	Whipple Shield

2. Materials and methods

2.1 Sample manufacturing

The impact tests were conducted on two types of target: a monolithic plate aluminum alloy 7075 (Aluminum) and a WS type structure with a composite material bumper (multilayered structure). The composite materials are manufactured by integrating several layers of Kevlar fabrics and carbon fiber ply within a polymeric matrix (epoxy resin) also reinforced by carbon nanotubes at 1wt% versus the matrix. The polymeric matrix is the bi-component epoxy resin Sika Biresin CR82 with the hardener CH 80-2 with density 1.15 g/cm^3 and viscosity 600 mPas at 25° C. The MWCNTs are the NC7000 (average diameter around 9.5 nm, average length 1.5 μm, purity 90%, surface area 250-300 m^2/g) supplied by NANOCYL. The layered carbon fiber reinforced polymer (CFRP)+Kevlar structure is made of six layers of carbon fiber (biaxial woven roving 0°-90°) and two of Kevlar fabrics. Manufacturing is performed by taking care to overlap one layer upon the other by following the scheme (0°÷90°), (+45°÷ −45°), (0°÷90°), two layers of biaxial

Kevlar fabric, and again three layers of carbon fiber as above. Fig. 1 shows a scanning electron microscope (SEM - TESCAN Vega 3LMH) picture of the employed MWCNTs and the fabrics used to build the layered CFRP+Kevlar structure. CNTs were homogeneously dispersed in the epoxy resin which was adopted to build the Kevlar and carbon fiber layered composite materials. Before mixing within the polymer matrix, the carbon nanomaterial was treated by sonication at room temperature in excess of ethanol. The sonication is carried out at 20 kHz for about 6 hours by means of Sonics Ultrasonicator (VCX750 model). After this preliminary step, the resin is added to the alcoholic solution in such amount to have the desired MWCNT concentration in the final composite; the composite mixtures realized consist in epoxy resin with inclusion of MWCNTs at 1wt% versus the matrix. The liquid compound is stirred for about 1 h at room temperature, and then put in oven at ~ 60 °C till the total evaporation of the solvent (typically it takes ~48 h), finally an aminic hardener is added and mixed. The layers are resin impregnated by two-side brushing, and positioned on each other within a mold by following the designed sequence; then a pressure loading of about 3 bar is applied over a rectangular zone (30 x 20 cm^2) of the as-packaged multilayer, finally the curing process is carried on in oven (16 h at 55 °C + 3h at 70 °C). In Fig. 2 several steps of the MWCNTs mixing within the polymer matrix and layered CFRP + Kevlar structures manufacturing are shown.
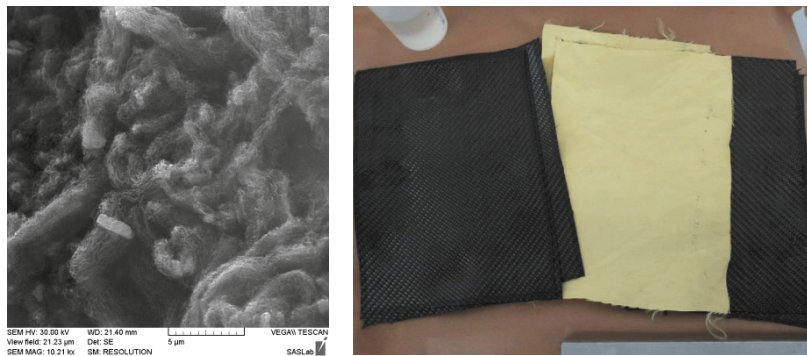

Fig. 1. SEM picture of MWCNT pristine material (left) and Carbon fibers and kevlar materials used to manufacture the nano-reinforced composite multilayer tile (right).
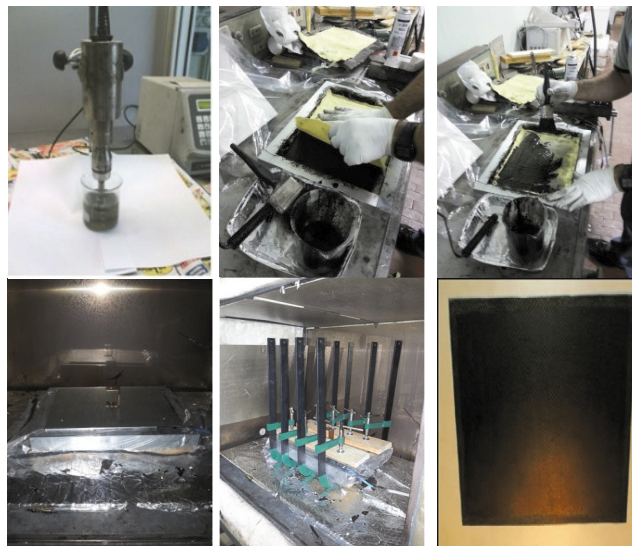

Fig. 2. Above, from left to right: sonication of the mixture MWCNT+ Resin , manufacturing of layers by using carbon fiber, kevlar and resin reinforced with carbon nanotubes at 1wt%; below: preform lid and pressure application, final nano-reinforced composite multilayer tile.
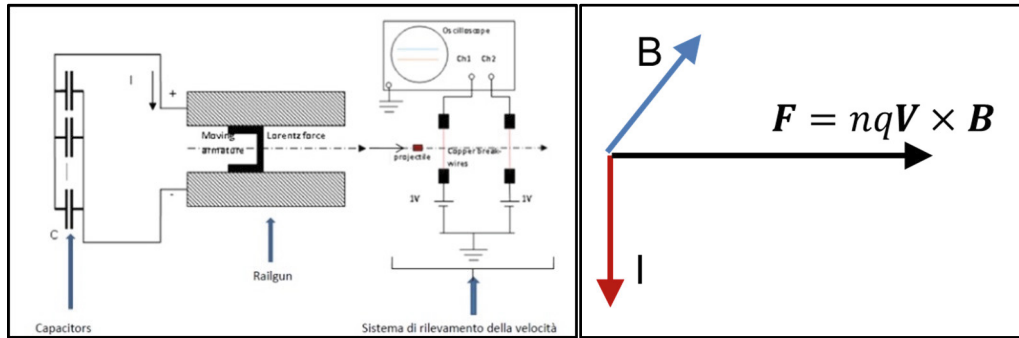
Fig. 3. Left: Railgun scheme, with the bank of high voltage capacitors for impulse discharge electrically connected to the rails and the Break-wire system for the bullet velocity measurement; right: Lorentz force representation.
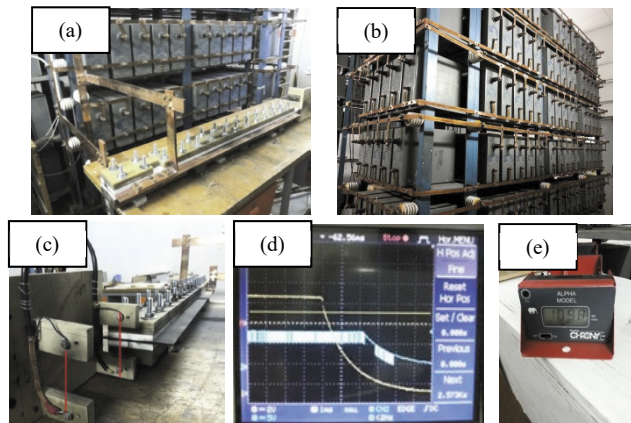

Fig. 4. (a) Railgun, (b) bank of the high voltage capacitors, (c) BWS, (d) Oscilloscope, (e) digital ballistic chronograph.

2.2 Railgun description

An new advanced electromagnetic launcher called railgun has been designed and realized in order to perform the debris impact study. In Fig. 3 the basic scheme of the railgun is shown. There are two parallel barrels (the rails), a moving armature (the bullet) and the electrical assembly of electrodes and capacitors deputed to energy storing and supply. The railgun is 1.40 m length, the rail bars are 5mm thick and 15mm spaced, and are electrically connected to a bank of 160 high voltage capacitors (6000 V, 72 mF) for an overall equivalent capacitance of about 11520 mF. Each capacitor has been supplied by ICAR S.p.A. INDUSTRIA CONDENSATORI (such capacitors were used in the past for the 'HotShot' system to test and study materials in plasma wind tunnel under high temperature plasma wind, with the aim to simulate the Earth's atmosphere reentry conditions). The capacitors can be charged up to 6000 V for a theoretical overall stored energy around 260 kJ. A tunable power supplier is used to set the capacitors charging voltage at the desired level: by this way the energy of the railgun can be easily tuned as a function of the desired bullet velocity. A great effort has been provided in order to achieve a reasonable high level of ballistic test reproducibility, mainly for what concerns the control of the railgun bias parameters and their influence on both values and statistical dispersion of the output energy. The break wire system (BWS) and a digital ballistic chronograph were used to measure the projectile velocity, as schematically shown in Fig. 3. The BWS consists of two thin copper strings stretched along the trajectory of the bullet and connected to a double power supply with two oscilloscope channels. When the projectile breaks up these copper conductors, the oscilloscope shows the voltage exponential decay at the two channels: the projectile velocity can be computed by taking into account of the elapsed time and the traveled distance. The pictures

in Fig. 4 show the railgun connected to the high voltage capacitors, the break wire system connected to the oscilloscope and the digital ballistic chronograph. The rails are mounted on a dielectric support mechanically resistant to the strong solicitations during the firing phase. In particular, the material supporting the projectile course is Teflon 15 mm thick while the rest of mechanical support is made of Vetronite type G10. Stainless steel screws of diameter 15 mm are used for the railgun assembly, while the electrical connection to the bank of capacitors is achieved by means of copper bars having section of 15 x 50 mm^2, held together by copper screws. These apparently over dimensioned electric conductors are required to withstand the sharp high current pulses (hundreds of thousand A).

Fig. 5. Left: Aluminum plate target; right: Whipple Shield target with CFRP + Kevlar tile bumper.

Fig. 6. At left the rail gun at rest and ready to fire; at centre, the image disturbed by the electromagnetic impulse (EMP); at right firing of the railgun with plasma jet.

3. Results and discussion

In this paper two of the several impact tests performed are reported: the first was carried out on the monolithic aluminum plate with a thickness of 5 mm at a velocity of about 650m/s, while the second was performed on an experimental setup that follows the configuration of a Whipple shield, with a first impact surface (bumper) made of CFRP + Kevlar and a subsequent plate (whitness plate) made of aluminum (Fig. 5). This second test was performed at a speed of about 1100 m/s. The projectile is made of Aluminum with a weight of about 5g; its mass is reduced of about 30% during the ballistic test. A sequence of three pictures showing railgun firing is reported in Fig. 6. In the first one the rail gun is at rest and ready to fire. In the second the image is disturbed by the electromagnetic impulse (EMP) generated by the current at firing instant. The last picture shows the firing of the railgun with plasma jet outgoing the railgun and directed to the target. In Fig. 7 some results of the ballistic tests performed on the first target made of Aluminum and on the manufactured composite tiles made of CFRP+Kevlar+CNT are shown. In the first case the target is completely perforated by the projectile at a speed of about 650 m/s; in the second case the bullet pierces the first plate made of CFRP+Kevlar+CNT (Bumper) and ends its run against the witness plate located behind, causing a bulge on the rear face. In the following images (Fig. 8 and Fig 9) some representations of the simulations carried out for each ballistic test described above are given. The firing tests have allowed us to verify the characteristics of railgun designed and manufactured for the study of the impacts of space debris. In the first test the capacitors have been charged to a voltage of about 3000 V for a stored energy around 52 kJ, while in the second test the capacitors have charged to a voltage of 4500 V for a stored energy around 116 kJ. The increment of projectile velocity from first to second test was considerable; whereas the capacitors can be charge up to 6000 V we can expect further strong increases in the launch speed of the projectile by the railgun.
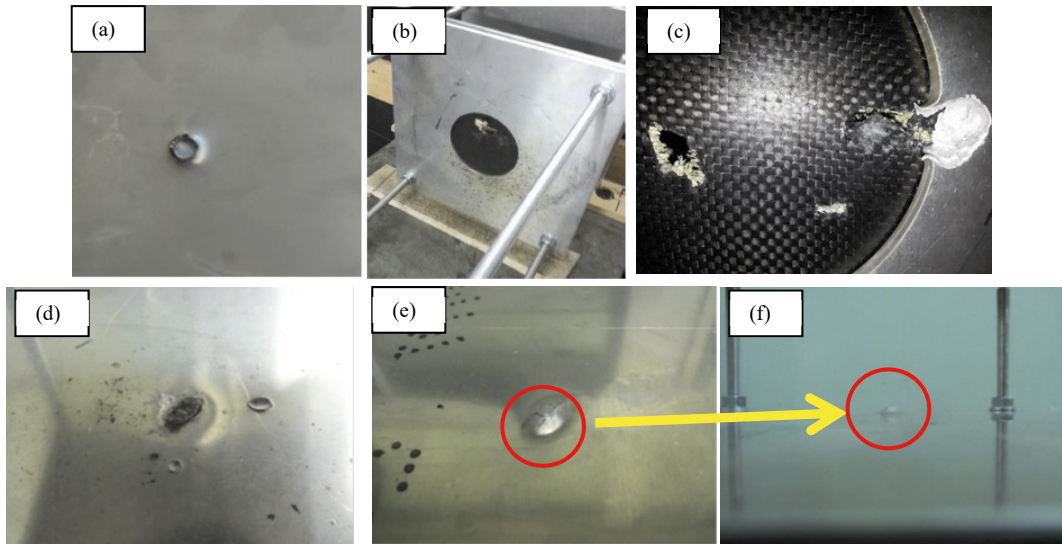
Fig. 7. (a) Perforated aluminum plate; (b) and (c) tiles made of CFRP+Kevlar+CNT after the test ; (d) the projectile stuck in the front face of witness plate; (e) and (f) bulge on the rear face of the witness plate.

In the following images (Fig. 8 and Fig 9) some representations of the simulations carried out for each ballistic test described above are given. The finite element model was prepared with a 3D drawing tool in which the impacting body is drawn similar to those used in the experimental impact test. The 3D sketch was later imported into solver and converted into a FEM model by applying the initial and boundary conditions. It has also taken steps to make a comparison between the measured weight and that calculated, starting from the geometric volume and the density of materials (found in the technical literature), by means of the evaluation function of the 3D design software. The imported geometry in the environment of the solver work was subsequently discretized into three-dimensional elements compatible with the explicit type analysis. The choice of the minimum dimensions of the elements, and then the level of detail of the mesh was dictated by the need to bring the solution to converge and the optimization
of times of calculation by imposing the Condition Courant-Friedrichs-Levy on the time step (1), as reported by S. Ma, X. Zhang , X.M. Qiu (2009).
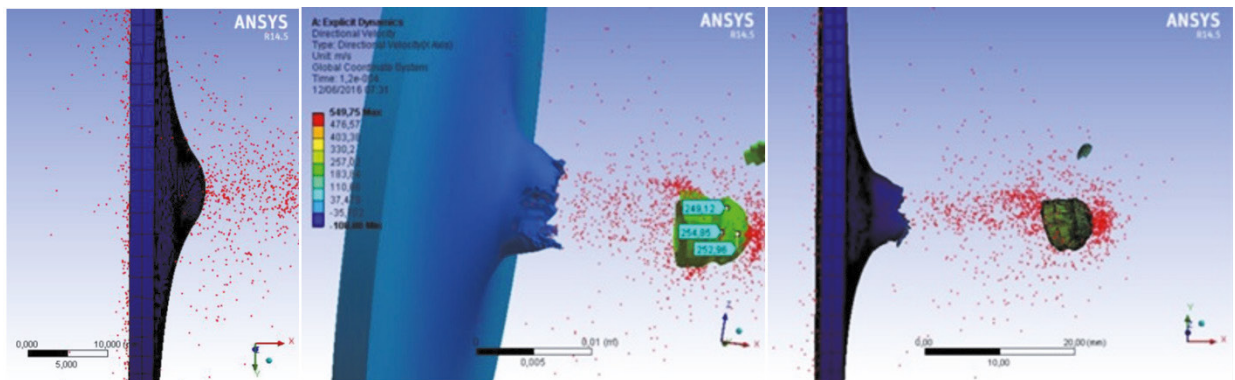

Fig. 8. From left to right: sequence of the numerical simulation of the first test.

$$\Delta t \le f \left[\frac{h}{c} \right]_{min} \tag{1}$$

where:
- *f* is the coefficient called "Stability time step-factor", generally between 0.6 and 0.9;
- *h* is the characteristic dimension finite element mesh;
- *c* is the velocity of wave propagation in the impacted material

Conclusions

Objective of the work was to report the recent results of ballistic test conducted in lab-environment by means of an in-house built electromagnetic accelerator device (rail gun) developed to perform impact test in space debris energy range. in order to explore different situations in terms of bullets energy and typology have been analyzed. The results obtained so far (the "perfect" match between the numerical simulations and the impact test results) have suggested the soundness of the proposed solution: such approach could represent the way forward in order to assess a competitive testing procedure for ballistic testing. A deeper analysis will be conducted in the next step of the research in order to develop an appropriate numerical model of the ballistic impact upon naked and micro/nano-reinforced composites. Further investigations will be carried out in order to achieve a deeper knowledge about the complex phenomena involved during an high energy impact upon multi-layered composite materials, with the aim to gain the possibility to design and realize the optimal combination of lightweight and ballistic resistant structures for anti-debris applications.
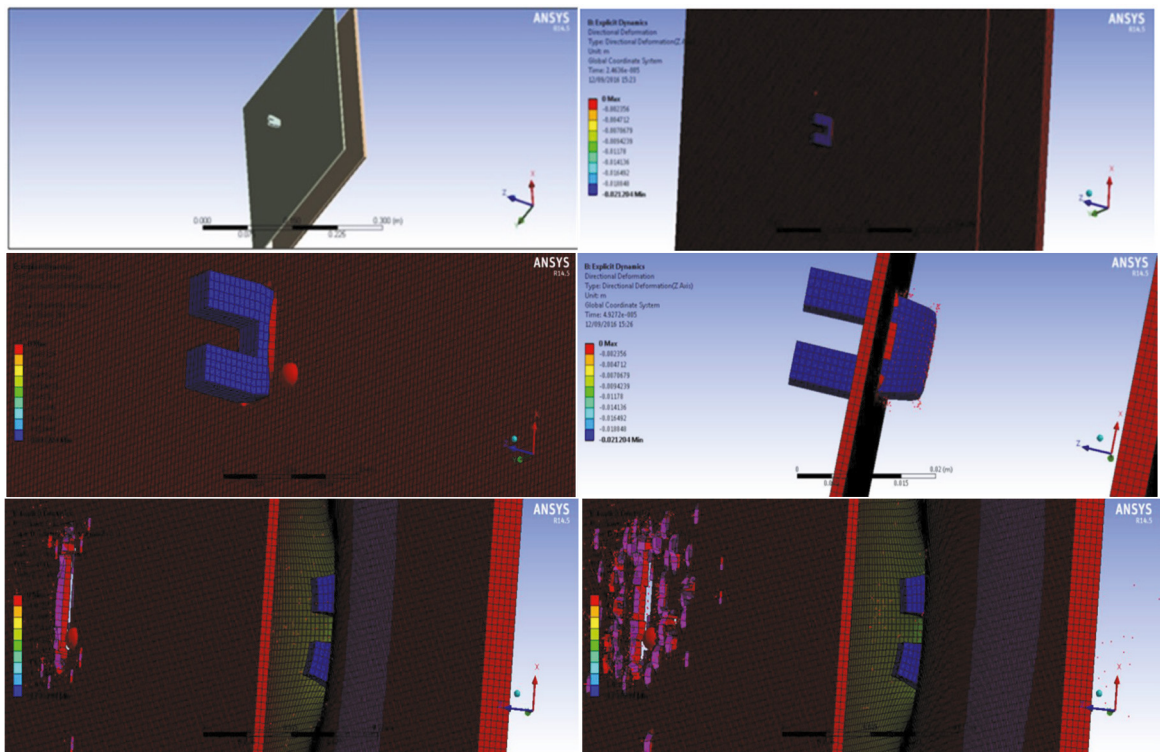
Fig. 9. Sequence of the numerical simulation of the second test.

References

McKnight, D.S., Dueber, R.E., Taylor, E.W., 1991. Space debris and micrometeorite events experienced by WL Experiment 701 in prolonged low Earth orbit. J. Geophys. Res.: Space Physics, 96(A6), 9829-9833.

Micheli, D., Vricella, A., Pastore, R., Albano, M., Marchetti, M., Gradoni, G., Moglie, F., Mariani Primiani, V., 2014. Railgun test of nano-reinforced layered composite materials for ballistic impact and electromagentic shielding. 54th Israel Annual Conference on Aerospace Sciences.

Micheli, D., Vricella, A., Pastore, R., Delfini, A., Giusti, A., Albano, M., Marchetti, M., Moglie, F., Primiani, V.M., 2016. Ballistic and electromagnetic shielding behaviour of multifunctional Kevlar fiber reinforced epoxy compo-sites modified by carbon nanotubes. Carbon.

Piattoni, J., Ceruti, A., Santoni, F., 2014. Automatic image analysis for space debris measurement. Proceedings of the International Astronautical Congress, IAC 2014.

Piergentili, F., Ceruti, A., Rizzitelli, F., Cardona, T., Battagliere, M.L., Santoni, F., 2014. Space debris measurement using joint mid-latitude and equatorial optical observations, IEEE Transactions on Aerospace and Electronic Systems.

Pigliaru, L., Borriello, C., Piergentili, F., Santoni, F., Pituccio, S., Pensavalle, E., 2014. Expanded polyurethane foam for active debris removal. Proceedings of the International Astronautical Congress, IAC 2014.

Santoni, F., Piergentili, F., Ravaglia, R., 2013. Nanosatellite cluster launch collision analysis", Journal of Aerospace Engineering.

Schneider, E., Stilp, A., Bureo, R., Lambert, M., 1990. Micrometeorite and space debris simulation for columbus hull components, Int. J. Impact Eng., 10, 499-508.

Palmieri, D., Faraud, M., Destefanis, R. Marchetti, M., 2001. Whipple shield ballistic limit at impact velocities higher than 7 KM/S International Journal of Impact Engineering, 26 (1-10), 579-590.

Eric, L., Christiansen, J., Kerr, H., 2001. Ballistic limit equations for spacecraft shielding, International Journal of Impact Engineering. 26(1–10), 93-104. http://dx.doi.org/10.1016/S0734-743X(01)00070-7.

Micheli D., Gradoni, G., Pastore, R., Apollo, C., Marchetti, M., 2010. Ballistic characterization of nanocomposite materials by means of Coil Gun electromagnetic accelerator, 19th International Conference on Electrical Machines,TPC-6 Theory Modeling and Design ICEM 2010, art. no. 5607827, IEEE Internat. Electronics Society (IEE) September 2010 Rome.

D. Micheli, R. Pastore, C. Apollo, M. Marchetti, 2011. Coil Gun electromagnetic accelerator for aerospace material anti-ballistic applications, Proc. of XXI CEAS-AIDAA Conference Venezia.

Faraud, M., Destefanis, R., Paimieri, D., Marchetti, M., 1999. SPH simulations of debris impacts using two different computer codes. Int. J. lmpactEngng. 23, 249-260.

Ma, S., Zhang, X., Qiu, X.M., 2009. Comparison study of MPM and SPH in modeling hypervelocity impact problems; International Journal of Impact Engineering, 36(2), 272–282; http://dx.doi.org/10.1016/j.ijimpeng.2008.07.001.